

Genome-Wide Identification of GH3 Genes in Brassica Oleracea and Identification of a Promoter Region for Anther-Specific Expression of a GH3 Gene

Hankuil Yi (✉ hankuil.yi@cnu.ac.kr)

Chungnam National University <https://orcid.org/0000-0002-9951-7856>

Jiseong Jeong

Chungnam National University

Sunhee Park

Chungnam National University

Jeong Hui Im

Chungnam National University

Research article

Keywords: B. oleracea var. oleracea, TO1000, Gretchen Hagen 3, GH3, anther, promoter

Posted Date: August 20th, 2020

DOI: <https://doi.org/10.21203/rs.3.rs-58799/v1>

License:   This work is licensed under a Creative Commons Attribution 4.0 International License.

[Read Full License](#)

Version of Record: A version of this preprint was published on January 6th, 2021. See the published version at <https://doi.org/10.1186/s12864-020-07345-9>.

Abstract

Background:

The *Gretchen Hagen 3* (*GH3*) genes encode acyl acid amido synthetases, many of which have been shown to modulate the amount of active plant hormones or their precursors. *GH3* genes, especially Group α subgroup 6 *GH3* genes, and their expression patterns in economically important kale-type *Brassica oleracea* have not been systematically identified.

Results:

As a first step to understand regulation and molecular functions of Group α subgroup 6 *GH3* genes, thirty-four *GH3* genes including four subgroup 6 genes were identified in *B. oleracea* var. *oleracea*, using TO1000. Synteny found around subgroup 6 *GH3* genes in TO1000 and Arabidopsis indicated that these genes are evolutionarily related. Although expression of four subgroup 6 *GH3* genes in TO1000 is not induced by auxin, gibberellic acid, and jasmonic acid, the genes show different organ-dependent expression patterns. Only one TO1000 subgroup 6 *GH3* gene, *Bo2g011210*, is expressed in anthers when microspores, polarized microspores, and bicellular pollens are present, similar to two out of four syntenic Arabidopsis subgroup 6 *GH3* genes. Detailed analyses of promoter activities of *Bo2g011210* further showed that *Bo2g011210* is expressed in tapetal cells and pollens in anther, and also expressed in leaf primordia and floral abscission zones.

Conclusions:

Sixty-two base pair (bp) region (-340 ~ -279 bp upstream from start codon) and about 450 bp region (-1489 to -1017 bp) in *Bo2g011210* promoter were found to be important for expressions in anther and expressions in leaf primordia and floral abscission zones, respectively. The identified anther-specific promoter region will be useful to develop male sterile transgenic *Brassica* plants.

Background

The *Gretchen Hagen 3* (*GH3*) gene was first identified in *Glycine max* (soybean) as an early response gene, which is transcriptionally induced less than 30 min by auxin plant hormone [1]. Later studies have found that *GH3* genes are found in diverse plant species including mosses and fern, but not in two model algae, *Chlamydomonas reinhardtii* and *Volvox carteri* [2–7]. Like acyl CoA synthetases, non-ribosomal peptide synthetases, and luciferases in ANL superfamily proteins, *GH3* proteins conjugate combinations of amino acids and acyl acids in two-step reactions [8–9]. In the first half-reaction involving ATP and acyl acid, adenylated acyl acid is produced and pyrophosphate is released. In the second half-reaction, adenylated acyl acid intermediate reacts with amino acids, resulting in the release of acyl acid-amino acid amido conjugate and adenosine monophosphate. For example, *Arabidopsis thaliana* (*Arabidopsis*) *GH3.11*, jasmonate (JA) resistant 1 (*JAR1*), and *Arabidopsis GH3.17*, reversal of sav 2 (*VAS2*), catalyzes the production of JA-isoleucine and indole acetic acid (IAA) – glutamate, respectively [10, 11].

GH3 proteins are involved in various developmental processes and environmental responses in plants, by modulating the activities or availabilities of plant hormones and related compounds, including precursors of plants hormones [12]. Abnormal expressions caused by null mutation or hyper- and mis-expression lead to various phenotypic defects. In Arabidopsis, *jar1* mutant does not produce bioactive JA-Isoleucine and defective in JA signaling, while *vas2* mutant over-accumulate free IAA at the expense of IAA-glutamate [11, 13]. In addition, Arabidopsis *avrPphB susceptible 3 (pbs3)* mutants were found to be more susceptible to bacterial pathogens because production of isochorismoyl glutamate, the precursor of salicylic acid (SA), catalyzed by PBS3, is compromised [14]. Over-expression of Arabidopsis *Dwarf in Light 1 (DFL1)* and *Yadokari 1 (YDK1)*, which are induced by auxin, causes hyper-sensitivity to light treatment leading to dwarfism [15, 16]. Over-expression of *WES1*, which is induced by treatment of abscisic acid and SA, as well as auxin, leads to auxin resistant phenotypes [17]. In various plants, important roles played by plant GH3 enzymes have also been demonstrated: nodule numbers and sizes in soybean [18], resistance to *Xanthomonas* bacteria in citrus [19], drought and salt tolerance in cotton [20], and fruit softening in kiwi and tomato [21], were shown to be affected by *GH3* gene expressions.

Phylogenetic analyses show that plant GH3 enzymes can be clustered into 3 groups (Group I~ III) based on overall amino acid sequences or 6 subgroups (subgroup 1 ~ 6) based on acyl acid-binding site sequences [7, 10, 12, 22]. However, only Group I and II *GH3* genes have been identified in Gramineae genomes [23–25]. Using GH3 enzymes in various plant species, preferential substrates of GH3 enzymes in terms of acyl acids and amino acids have been determined [8, 14, 18, 22, 26–30]. In addition, a systematic evaluation of sixty GH3 enzymes from Arabidopsis, grape, rice, Physcomitrella, and Sellaginella also revealed that not all the enzymes in Group I are involved in JA signaling and twelve out of sixteen subgroup II GH3 enzymes tested displayed clear substrate preferences for IAA using three acyl acid substrates - jasmonate, IAA, and 4 hydroxybenzoate (4-HBA) [31]. In case of Group II GH3 enzymes, which is the largest GH3 group in the genome, no clear substrate preferences could be established, except AtGH3.9 or OsGH3.13 for IAA and Arabidopsis PBS3 for 4-HBA. In addition, AtGH3.15 (At5g13350), another GH3 in Group II subgroup 6, was shown to have substrate preference for indole butyric acid (IBA), the auxin precursor [28]. Although decrease in IBA-mediated root elongation inhibition and lateral root formation were observed in transgenic plants constitutively expressing *AtGH3.15*, *in vivo* function(s) of subgroup 6 *GH3* genes are yet to be determined. In rapeseed (*Brassica napus*) and its diploid ancestors, Chinese cabbage (*Brassica rapa*) and cabbage (*Brassica oleracea* var. *capitata*), up to sixty six GH3-coding genes have been identified [32–33]. However, detailed study of GH3-coding genes in kale-type *Brassica* species (*Brassica oleracea* var. *oleracea*), TO1000, which serves as excellent model for important vegetable crops in *Brassica oleracea* with various morphological and phytochemical traits [34], have not been performed yet.

Anther is a part of stamen, the male reproductive organ in plants, and connected to flower receptacle by filament, the other part of stamen [35, 36]. Anther development is divided into two phases, culminating in the release of pollen grains, male gametophytes in plants. Microsporogenesis, the first phase, includes establishment of anther morphology, cell and tissue differentiation, and meiosis of microspore mother cells. Tetrads of haploid microspores produced by meiotic divisions of diploid pollen mother cells are

released as distinct unicellular microspores into locules, by a mixture of enzymes produced from tapetum cells, which provide nutrients and pollen wall materials for developing pollens as well [37, 38]. During microgametogenesis, the second phase, differentiation of microspores into pollen grains and tissue degeneration occur for release of pollens. Microgametogenesis starts with the expansion of the microspore, which is often found with the formation of one large vacuole [39]. This involves movement of the microspore nucleus from center of the cell to a position close to the cell wall, where the microspore produces two unequal cells, a large vegetative and a small generative cell, in a process called pollen mitosis (PM) I. Then, the generative cell, which is spatially separated from the pollen grain wall and engulfed by the vegetative cell, undergoes another round of cell division, called PM II [37]. Depending on whether the PM II happens before or after pollen dispersal from anther, the pollens are called tricellular or bicellular pollen [40]. Plant hormones – JA, auxin, gibberellic acid (GA), and ethylene – are known to play important roles in stamen maturation, locule opening, anther dehiscence, and pollen viability during stamen and pollen development [35, 41–43].

In this study, *GH3* genes in TO1000, kale-type *B. oleracea* var. *oleracea*, were identified genome-wide and expression patterns of subgroup 6 *GH3* genes, whose functions are still elusive, were investigated. It was found that TO1000 subgroup 6 *GH3* genes, composed of four genes showing synteny with closely related Arabidopsis subgroup 6 *GH3* genes, are not induced by auxin, GA, and JA treatment, but have different organ expression patterns. *Bo2g011210*, a subgroup 6 *GH3* gene in TO1000, is specifically expressed in tapal cells in anther and pollens when microspores, polarized microspores, and bicellular pollens are produced, as well as in leaf primordia and floral abscission zones. Promoter bash experiments revealed that sixty-two base pairs (bp) DNA sequence, -340 to -279 bp upstream of *Bo2g011210* start codon, is required for anther-specific expression, while about 450 bp region (-1489 to -1017) is necessary for expressions in leaf primordia and floral abscission zones.

Results

Thirty four GH3-encoding genes (BoGH3s) are present in TO1000

In Ensembl Plants database (<http://plants.ensembl.org/index.html>), protein sequences of fifty five GH3 candidate genes in TO1000, kale-type *B. oleracea*, showed similarities to the nineteen Arabidopsis GH3 proteins [10]. Among these, thirty four GH3 proteins were found to have intact GH3 domains (pfam03321) and considered as GH3 proteins (Table S1; Figure S1). Although identical genomic sequence was also used for annotation in NCBI database (NCBI, <http://ncbi.nlm.nih.gov>) [34], only thirty *B. oleracea* GH3 candidate proteins, including two with truncations in GH3 domains, were found to have significant similarities to Arabidopsis GH3s. The thirty four BoGH3 proteins with the intact GH3 domains in Ensembl Plants database include all twenty eight putative GH3 proteins with the intact GH3 domains identified in NCBI database (Table S1). For proteins showing different protein sequences between two databases, such as Bo3g009110 and Bo5g053450, NCBI protein models were adopted in our study because they are supported by RNA-seq data in NCBI. While thirty four GH3 protein-coding genes were identified from kale-type TO1000 (*B. oleracea* var. *oleracea*) in our study, twenty five and twenty nine GH3 protein-coding

genes were previously reported for cabbage type *B. oleracea* var. *capitata* in the comparison with *B. napus* genes by two independent studies, respectively [32, 33].

Similar to previous phylogenetic analyses of GH3 proteins including cabbage type *B. oleracea* var. *capitata*, phylogenetic clustering of Arabidopsis and BoGH3 proteins demonstrated that BoGH3 proteins can be divided into 3 groups (Group I, II, and III) (Fig. 1A) [6, 10, 32, 33]. It was found that Group I consists of two Arabidopsis and four BoGH3 proteins, while Group II consists of eight Arabidopsis and eleven BoGH3 proteins. In case of Group III, nine Arabidopsis GH3s and nineteen BoGH3 proteins were clustered together. In general, exon/intron structures of *BoGH3* genes were same to closely related counterparts in Arabidopsis with some exceptions (Fig. 1B). For example, four protein-coding exons were detected for *Bo9g023750* in Group III, based on the distribution of RNA-seq reads in NCBI database, while three protein-coding exons of *At2g14960* is reported in TAIR JBrowse (<https://jbrowse.arabidopsis.org/>). In case of *Bo3g039200* and *Bo4g196110*, which are closely related to *At2g46370* (*JAR1*) with four protein-coding exons, three exons supported by RNA-seq reads were observed. Structural differences were also observed for five *BoGH3* genes (*Bo3g023700*, *Bo4g164910*, *Bo7g116230*, *Bo7g011450*, and *Bo8g109490*) that were identified only in Ensembl Plants.

Synteny is observed for Group III subgroup 6 GH3 genes in Arabidopsis and TO1000

In TO1000, four out of thirty four Group III BoGH3 proteins (*Bo2g011200*, *Bo3g009140*, *Bo7g011450*, *Bo9g166800*) show a close relationship with Arabidopsis subgroup 6 GH3 (Fig. 1A). While these four *BoGH3* genes are found on different chromosomes, four Arabidopsis *GH3* genes (*At5g13350*, *At5g13360*, *At5g13370*, and *At5g13380*) in the same subgroup are located within less than 15,000 base pairs (bp) genomic region on Arabidopsis chromosome 5 (Fig. 2A). When genes located around Arabidopsis and TO1000 subgroup 6 *GH3* genes were compared, synteny was detected around the *At5g13350* ~ *At5g13380* *GH3* cluster and three TO1000 *GH3* genes (*Bo2g011210*, *Bo3g009140*, and *Bo9g166800*) (Fig. 2B-2D). In the upstream of three TO1000 *GH3* genes, *Bo2g011200* (Fig. 2B), *Bo3g009120* (Fig. 2C), and *Bo9g167820* (Fig. 2D) showing sequence similarities to *At5g13330*, an *RAP2.6L* transcription factor, which is found upstream of the *At5g13350* ~ *At5g13380* *GH3* cluster, were identified (Fig. 2A). Moreover, *Bo2g011190*, *Bo3g009110*, and *Bo9g167830*, which are clustered with *At5g13320* (*PBS3*) in the phylogenetic tree as Group III subgroup 4 *GH3* genes, were also found further upstream, same to *At5g13320* (*PBS3*) located upstream of the *At5g13350* ~ *At5g13380* *GH3* cluster. Consistent with the syntenic relationships in these genomic regions, sequence similarities were also observed downstream of the Arabidopsis *GH3* cluster and the three TO1000 *GH3* genes on different chromosomes (Fig. 2): *Bo2g011240* and *Bo9g166790* show sequence similarity to *At5g13390*, *No Exine Formation 1*.

Subgroup 6 BoGH3 genes are not induced by auxin treatment in the seedling stage

In Arabidopsis, auxin treatment can induce transcription of some *GH3* genes, such as *At4g27260* (*WEST1*), *At4g37390* (*YDK1*), and *At5g54510* (*DFL1*) [15–17]. However, expression conditions and functions of *GH3* genes in other plants are largely unknown. To gain insights on the expression patterns and functions of four TO1000 subgroup 6 *GH3* identified in this study, we determined whether these genes can be

induced by plant hormones and found that none of subgroup 6 *BoGH3* genes were significantly induced by auxin (synthetic 2,4-Dichlorophenoxy acetic acid (2,4-D) or natural IAA), GA or JA treatment at the seedling stage, except *Bo3g009140* that is weakly induced by JA (Fig. 3). However, transcriptional inductions by auxin were evident for *Bo1g004760*, a *YDK1*-like *BoGH3* gene, and *Bo1g048130*, a *WES1*-like *BoGH3* gene, like their closely related *GH3* genes in Arabidopsis [16, 17].

Bo2g011210 and Bo1g048130 are strongly expressed in stamen at a specific stage during flower development

For four subgroup 6 and two auxin-inducible *GH3* genes in TO1000, relative expression patterns in six different organs - root, leaf, stem, floral bud, opened flower, and silique - were determined. Among four subgroup 6 *BoGH3* genes, *Bo2g011210* was found to be most strongly expressed in floral bud, although significant expression was observed in silique compared to that in leaf (Fig. 4A). Only negligible expressions of *Bo2g011210* were detected in other organs, including open flowers. For the other three subgroup 6 *BoGH3* genes, the strongest expression was commonly found in siliques (Fig. 4B-4D), while comparable expressions in floral bud and open flower were also observed for *Bo3g009140* (Fig. 4B). For auxin-inducible *Bo1g004760* and *Bo1g048130*, distinct relative expression patterns were detected: *Bo1g004760* and *Bo1g048130* were found to be most strongly expressed in root and floral bud, respectively (Fig. 4E & 4F).

For *Bo2g011210* and *Bo1g048130*, which show strong preferential expressions in floral bud (Fig. 4A & 4F), it was also determined whether expressions of these genes are temporally regulated during floral bud development. When the expression levels were monitored for developing floral buds sorted by lengths, which reflect the progress of flower development [44], both genes showed stronger expression when bud lengths are about 2 to 6 mm, although *Bo2g011210* in subgroup 6 *GH3* showed more dramatic expression changes by developmental progress than *Bo1g048130* (Fig. 5A & 5B). In 4 ~ 6 mm-long floral buds, where the two genes are most strongly expressed, almost exclusive expression was detected in stamen among sepal, petal, stamen, and pistils (Fig. 5D & 5E). In contrast, no significant developmental and organ-specific expression patterns were observed for *Bo3g009140*, another subgroup 6 *BoGH3* (Fig. 5C & 5F).

Bo2g011210 and Bo1g048130 are expressed in tapetum and pollen grains

To narrow down spatial expression patterns of stamen-expressed *Bo2g011210* and *Bo1g048130*, we generated transgenic plants, in which *GUS* (β -glucuronidase) reporter genes are expressed under the control of about 1,500 bp putative promoter sequences of these *BoGH3* genes. *Bo2g011210* (-1489 ~ -1)::*GUS* and *Bo1g048130* (-1496 ~ -1)::*GUS* are two transgenic plants, in which -1489 ~ -1 and -1496 ~ -1 bp DNA sequences upstream of *Bo2g011210* and *Bo1g048130* start codon, respectively, are fused to *GUS* reporter genes. In *Bo2g011210* (-1489 ~ -1)::*GUS*, *GUS* expression was observed in anthers of developing floral buds (Fig. 6F & 6G), consistent with the qRT-PCR (quantitative reverse transcription polymerase chain reaction) results (Figs. 4 & 5). Weak *GUS* staining in some stigmas was found to be caused by stigma-attached pollens (Fig. 6H). *GUS* staining was also observed in siliques, but only in the

floral organ abscission regions of petals, sepals, and stamens (Fig. 6I & 6J). In addition, GUS expression was detected in leaf primordia of seedlings (Fig. 6K & 6L). In *Bo1g048130* (-1496 ~ -1)::GUS, GUS expression was detected in developing anthers and unfertilized ovule or aborted seeds (Fig. 6M – 6Q), but not in seedling leaf primordia (Fig. 6R). To further define the spatial expression patterns of *Bo2g011210* and *B1g048130* in anther, cross-sectioned floral buds were examined and specific expression in tapetum cells and pollen grains were detected (Fig. 6U – 6X). In *Bo2g011210* (-1489 ~ -1)::GUS, GUS staining seems to appear in the tapetum first and pollens later (Fig. 6U & 6V).

Bo2g011210 and B1g048130 are most strongly expressed around when polarized microspores are generated

To investigate which milestone events in microsprogenesis or microgametogenesis occur in pollens when *Bo1g048130* and *Bo2g011210* are expressed (Fig. 5), developing pollens were collected from floral buds and open flowers. Based on the numbers and organization of 4',6-diamidino-2-phenylindole (DAPI)-stained nuclei, it was found that tetrads and microspores are observed in less than 2 × floral buds (Fig. 7A & 7D), in which the two anther-expressed *GH3* genes, *Bo2g011210* and *Bo1g048130*, are weakly expressed (Fig. 5). In 2 ~ 6 × floral buds, in which the two anther-expressed *GH3* genes are most strongly expressed, microspores, polarized microspores, and bicellular pollens were observed (Fig. 7B – 7C & 7E – 7F). While bicellular and tricellular pollens were observed in 6 ~ 8 × buds, only tricellular pollens were observed in 8 ~ 10 × buds and opened flowers (Fig. 7G – 7L). These data show that *Bo2g011210* and *Bo1g048130* are strongly induced when polarized microspores are mainly produced during early microgametogenesis [45, 46].

One hundred eighty six bp region upstream of Bo2g011210 is sufficient for anther-specific expression

DNA sequences responsible for tissue-specific expression of *Bo2g011210* was investigated with different DNA regions upstream of the start codon (Fig. 8A). When P1 region, in which -1017 ~ -1 bp region was fused upstream of *GUS* reporter gene, was used to generate *P1* transgenic plants, *GUS* expressions in anthers and pollens were still detected (Fig. 8B – 8D), but those in floral abscission zones and leaf primordia were lost, except one case showing GUS staining in the floral abscission zone (Fig. 8E & 8F). When P2 (-418 ~ -1) and P3 (-340 ~ -155), in which -155 ~ -1 bp 5' untranslated region based on RNA-seq reads in SRX209697 (NCBI) is removed, were used, anther-specific *GUS* expressions were found to be maintained (Fig. 8G & 8H). While *P4* (-278 ~ -155) did not show *GUS* expression in all twelve lines, five out of twelve *P5* (-418 ~ 279) showed *GUS* expression, suggesting sixty-two bp region (-340 ~ -279) in P3 sequence is important for anther-specific expression of *Bo2g011210* (Fig. 8I & 8J).

Discussion

Thirty four *GH3*-coding genes of TO1000, kale-type *B. oleracea* (var. *capitata*), which have intact *GH3* domains, were identified from Ensembl plants database (Fig. 1A). Among these, twenty eight gene models were also found in NCBI database, which had used the identical genomic sequence for annotation [34]. The discrepancy in *BoGH3* gene numbers between Ensembl plants and NCBI database

may result from the use of different gene prediction algorithms or validations. Recently, twenty five or twenty nine GH3 protein-coding gene models originating from cabbage-type *B. oleracea* var. *capitata* were identified from the investigation of genomic sequence of *B. napus* [32, 33]. Out of twenty nine *B. napus* GH3 genes with *B. oleracea* var. *capitata* origin, twenty eight genes were found to have intact GH3 domains and meet our criteria, while *BoI042635* was found to encode a truncated GH3 domain with 224 amino acids (Table S4) [33]. Among thirty four BoGH3 coding-genes reported in this study, putative orthologs of cabbage-type *B. oleracea* were identified for nineteen genes, but clear orthologous relationship could not be determined for the other fifteen TO1000 GH3 genes, based on amino acid sequence identities of over 95%. Considering six out of BoGH3 genes, whose expression could not be confirmed in NCBI database, are included in these fifteen cabbage-type GH3 genes without putative orthologs, we speculate these six genes are pseudogenes and lost in *B. oleracea* var. *capitata*. In addition, orthologs of nine cabbage-type *B. oleracea* GH3 genes could not be determined in TO1000 (Table S4).

Group III subgroup 6 GH3 genes in TO1000 and Arabidopsis seem to have evolved by duplications. Four Arabidopsis GH3 genes in subgroup 6 are located within 15 kbp region on the same Arabidopsis chromosome, while four BoGH3 genes in the same subgroup are located on 4 different TO1000 chromosomes (Fig. 2). Synteny found between genomic regions around the Arabidopsis and TO1000 genes suggest that *At5g13350~At5g13380* GH3 cluster in Arabidopsis was generated by tandem duplication after *Brassicaceae* lineage-specific whole genome triplication and/or other TO1000 GH3 genes around *Bo2g011210*, *Bo3g009140*, and *Bo9g166800* GH3 genes might have been lost after divergence of *Arabidopsis* and *Brassicaceae* lineages [47]. One intact and one truncated GH3 genes in subgroup 6, *Bo2g011210* and *Bo2g011230*, were identified within 15 kb region on the TO1000 chromosome 2 (Fig. 2B). Members in gene family in plants have evolved through both tandem (local) duplication and whole genome duplication, which were followed by gene loss or gene retention leading to functional diversification [48]. Nonetheless, close genomic locations of subgroup 4 and subgroup 6 GH3 genes in Arabidopsis and TO1000 indicate both *At5g13320-like* and *At5g13350-like* GH3 genes were present before the separation of *Arabidopsis* and *Brassica* lineages. For exon/intron structures of TO1000 and Arabidopsis GH3 genes, overall similarities were generally observed for the evolutionarily related genes. However, distributions of RNA-seq reads in NCBI database revealed that protein-coding exons of *Bo9g023750*, *Bo3g039200*, and *Bo4g196110* are differently organized compared to those of related Arabidopsis GH3 genes (Fig. 1B). Differences in the structures observed for five TO1000 GH3 genes (*Bo3g023700*, *Bo4g164910*, *Bo7g116230*, *Bo7g011450*, and *Bo8g109490*) and related Arabidopsis genes might result from incorrect annotations, considering that these five TO1000 genes are identified only in Ensembl Plants, not supported by RNA-seq data in NCBI database, and encode predicted GH3 proteins with multiple deletions (Fig. 1B, Figure S1).

Four subgroup 6 BoGH3 genes, which seem to be generated from same ancestor gene(s), show distinct expression patterns. At the organ level, *Bo2g011210* is almost exclusively detected in floral buds by qRT-PCR, while the strongest expressions of *Bo7g011450* and *Bo9g166800* are observed in siliques (Fig. 4A, 4C & 4D). In case of *Bo3g009140*, no significant expression preference is found among different TO1000 organs and constitutively expressed in all parts of flowers (Fig. 4B, 5C & 5F). In developing floral buds,

Bo2g011210 is strongly expressed in stamen when floral buds are about 2 ~ 6 mm long (Fig. 5). However, investigation of *Bo2g011210* promoter activity using GUS reporter revealed that *Bo2g011210* is also expressed in abscission zones in siliques and leaf primordia, in addition to tapetal cells in stamen and pollen grains (Fig. 6F – 6L). Relatively weak detection of *Bo2g011210* in siliques by qRT-PCR may be related to the facts that the gene is expressed only in smaller portions of siliques cells, although we do not exclude the possibility that the expression level is also lower in siliques than in stamen. In 2 ~ 6 mm floral buds, in which *Bo2g011210* is most strongly expressed, microspores, polarized microspores, and bicellular pollens are mainly observed in anthers (Fig. 7). Similar to *Bo2g011210*, two syntenic subgroup 6 Arabidopsis *GH3* genes, *At5g13380* and *At5g13350*, are expressed in flower stage 9 ~ 11 floral buds and flower stage 12, respectively [49]. More specifically, *At5g13380* is expressed in polarized microspore and *At5g13350* is expressed bicellular pollens. Based on the numbers of pollen nuclei and floral bud phenotypes [50], the T01000 flower stages, when *Bo2g011210* is strongly expressed, roughly correspond to stages 8 ~ 12 of Arabidopsis flower and overlap with the periods when *At5g13350* and *At5g13380* are expressed (Fig. 7 & S2). Although *Bo1g048130*, a group 6 *BoGH3* gene, is also specifically expressed in stamen like *Bo2g011210* (Fig. 3A – 3B & 6U – 6X), *Bo1g048130* seems to be expressed in a longer time period compared to *Bo2g011210* (Fig. 5A – 5B, 6H & 6O). Different from *Bo2g011210*, neither in floral abscission zones nor in leaf primordia is expression of *Bo1g048130* observed (Fig. 6P & 6R).

Bo2g011210 is not induced by auxin (IAA or 2,4-D), JA, or GA, but expressed in a tissue-specific manner. Since their first identification in soybean as early responsive genes to auxin [1], many *GH3* genes have been found to be induced by various plant hormones, such as auxin, SA, and JA [17, 33, 51, 52]. When hormone inducibility for auxin, GA, and JA was tested using whole seedlings, no expression changes for *Bo2g011210* and three other subgroup 6 *BoGH3* genes were detected in our experimental conditions (Fig. 3). In contrast, expression levels of *Bo1g004760* was found to be elevated upon exposure to auxin in the same condition. Similar to our findings, all subgroup 6 *GH3* genes in *B. napus*, an allotetraploid carrying *B. oleracea*-originated chromosomes, did not show any significant expression changes in response to IAA treatment to leaves [33]. Although *Bo2g011210* expression is not induced by auxin in our experimental condition, tissues or cells, in which *Bo2g011210* promoter activity is detected, partially overlap with the regions where auxin-responsive *DR5* promoter is activated in Arabidopsis and rice (Figs. 3 & 6) [53–56]. We do not exclude the possibility that *Bo2g011210* promoter is less sensitive to auxin treatment than *Bo1g004760*, but we prefer the idea that expression of *Bo2g011210* is induced by a transcription factor that is activated in tissue-specific manners downstream of auxin signaling pathway.

Anther-specific expression of *Bo2g011210* is directed by 62 bp DNA sequence, from – 340 to -279 bp from the start codon. Determination of promoter regions important for tissue-specific expressions revealed that about 180 bp P3 region (-340 ~ -155) close to the transcription start site is sufficient for anther-specific expression (Fig. 8). The observation that P4 region (-278 ~ -155) does not support anther-specific expression suggests that *cis*-acting element necessary for anther-specific expression is included in 62 bp DNA sequence from – 340 to -279 bp. GUS expression detected in five out of twelve P5 transgenic lines containing – 418 to -279 bp region further supported this idea. We suspect that deletion of promoter sequences (-278 ~ -155) close to the transcription start site makes anther-specific expression

depend on the genomic positions where transgene is inserted. In Arabidopsis, Male Sterility 1 plant homeodomain-finger and MYB99 transcription factors functioning in anther and pollen development pathway are expressed in microspores, polarized microspores, and bicellular pollens [49, 57]. The findings (1) that *Bo2g011210* is strongly expressed when microspores, polarized microspores, and bicellular pollens are produced and (2) that MYB core *cis*-acting element (CTGTTA) is located at -293 ~ -288 raises a possibility that TO1000 ortholog of Arabidopsis MYB99 play an important role for anther-specific expression of *Bo2g011210* [58]. Because *GUS* expressions in leaf primordia and floral abscission zones are lost without any obvious effect on anther-specific expression, *cis*-acting element important for leaf primordia and floral abscission zone expressions must be located in the - 1489 to -1017 region in *Bo2g011210* promoter and independent of that for anther-specific expression (Fig. 8A – 8F).

Conclusions

In this study, we identified anther-specifically expressed TO1000 *GH3* genes and critical promoter region for anther-specific expression. The information will broaden our understanding of transcriptional regulations during anther development and can be used to develop transgenic male sterile lines for economically important *Brassica* plants.

Methods

Plant growth

Brassica oleracea var. *oleracea* (TO1000 seeds, stock number CS29002) were obtained from Arabidopsis Biological Resource Center. TO1000 and Arabidopsis plants were grown on soil or a half-strength liquid Murashige and Skoog (MS) media (pH 5.7) with vitamins made with Duchefa Biochemie M0222 (Haarlem, Netherlands). Plants were grown under a 16 hours (hr) light/8 hr dark photoperiod at 22°C. TO1000 organ samples were collected from 50-day old soil-grown plants.

Transgenic Arabidopsis plants (ecotype Columbia) carrying β -glucuronidase (*GUS*)-coding sequences expressed by *GH3* promoter sequences were selected on half-strength solid MS media containing 0.8% Duchefa Plant agar P1001 (Haarlem, Netherlands) and 20 µg/ml Kanamycin, and transferred to soil for flowering.

Hormone Treatment

For hormone treatment, surface sterilized TO1000 seeds were germinated and grown in 24 well plates containing 1 ml half-strength liquid MS media for 5 days. 2,4-D (D0901), IAA (I0901), GA (G0907) and JA (J0936) from Duchefa (Haarlem, Netherlands) were treated to whole seedlings, after the seedlings were further grown in 2 ml fresh liquid media for 6 hr.

Sample Collection

Five-day-old seedlings were used to determine whether *BoGH3* gene of interest is induced by hormone treatment. For gene expression analysis by qRT-PCR, root, leaf, stem, floral bud, open flower, and silique were obtained from 3 individual plants: more specifically, eleventh to thirteenth leaves, fifth to seventh node for stems, a mix of unopened floral buds without white petals exposed (bud length less than about 8 mm), a mix of open flowers (bud length larger than 8 mm) with white petals exposed, and siliques with various sizes were collected. Samples for floral buds were further divided into 5 categories by lengths: 0 ~ 2, 2 ~ 4, 4 ~ 6, 6 ~ 8, and 8 ~ 10 mm sizes (Figure S2). Sepals, petals, anthers, and pistils were collected from 4 ~ 6 mm-long unopened floral buds. After collection, samples were frozen in liquid nitrogen and stored at -80 C° until RNA isolation. Samples for GUS staining were collected, when transgenic *Arabidopsis* seedlings were 8 days old or later when inflorescence and siliques were mature enough.

Identification of genes encoding putative GH3 family proteins in TO1000

To identify putative GH3-coding genes in TO1000, nineteen *Arabidopsis* GH3 protein sequences downloaded from The Arabidopsis Information Resource (TAIR, <http://www.arabidopsis.org/>) were used for BLAST search in Ensembl Plants database (<http://plants.ensembl.org/index.html>) and National Centre for Biotechnology Information (NCBI, <http://ncbi.nlm.nih.gov>). In Ensembl plants and NCBI database search, E-value thresholds for candidates were set on $1e^{-1}$ and 0.1, respectively. BoGH3 proteins were further determined by the presence of the intact GH3 domains, and their exon/intron structures were determined based on RNA-seq exon coverage and RNA-seq intron spanning reads from NCBI *B. oleracea* annotation Release 100. Similarly, GH3 protein sequences in *B. oleracea* var. *capitata* were identified using sequence in Bolbase (<http://ocri-genomics.org/bolbase/blast/blast.html>) [59].

Multiple Sequence Alignment And Construction Of Phylogenetic Tree

The multiple sequence alignment of GH3 proteins was performed using the Clustal Omega and visualized using Jalview [60, 61]. Phylogenetic analysis was performed using the molecular evolutionary genetics analysis (MEGA) software [62]. The evolutionary history was inferred by using maximum likelihood method based on the JTT matrix-based model [63]. All positions with less than 90% site coverage were eliminated. There were a total of 549 positions in the final dataset. Bootstrap test was repeated 1000 times.

Rna Isolation, Reverse Transcription, And Qrt-pcr Analysis

Total RNA was extracted using PhileKorea E-Zol RNA Reagent (Seoul, Korea) or Ambion TRIzol® Reagent (Austin, USA) following the manufacturer's instructions. For silique samples, Invitrogen Plant RNA Purification Reagent (Carlsbad, USA) was used to. cDNA was synthesized from RNA with 260/280 ratios

between 1.8 and 2.1. First strand cDNA was synthesized with Toyobo ReverTra Ace- α (Osaka, Japan) and 1.0 μ g of total RNA, according to the manufacturer's instructions. In case of hormone-treated seedlings, 0.5 μ g of total RNA was used. As described in Nam *et al.* (2019), qRT-PCR was performed with a two-step reaction: 3 minutes (min) at 95 °C, followed by 50 cycles of 10 seconds at 95 °C and 30 seconds at 60 °C. Primer sequences used are listed in Table S2. For each analysis, three technical replicates of at least two independent biological replicates were used.

Construction of GH3 promoter-GUS reporter vector and plant transformation

DNA regions upstream of the start codon of *GH3* genes used for promoter analyses are as follows: -1489 ~ -1, -1017 ~ -1, -500 ~ -1, -418 ~ -1, -340 ~ -155, -278 ~ -155 bp of *Bo2g011210*, and -1496 ~ -1 bp of *Bo1g048130*. Putative promoter regions were PCR-amplified with specific primers with Sall or BamHI recognition sequence for cloning (Table S3). After Sall and BamHI digestion, the PCR fragments were cloned into pBI101.1 vector between Sall and BamHI sites. The construct was transformed into *Arabidopsis* by floral dip method [64].

Histochemical GUS Staining And Paraffin Section Of GUS-stained Samples

Histochemical GUS staining was performed with 0.5 mg/ml MBcell 5-bromo-4-chloro-3-indolyl-beta-D-glucuronic acid-cyclohexylammonium salt (Seoul, Republic of Korea), as previously described [65]. The floral buds of T1 or T2 transgenic plants carrying a *GH3 promoter::GUS* fusion transgene were immersed in GUS reaction buffer in the dark condition for 1 day at 37 °C, then samples were washed in 95% ethanol for 1 ~ 2 hr. At least 7 individual transgenic lines were used to analyse GUS expression patterns.

To perform paraffin section, GUS-stained samples were fixed in FAA solution (Formaline : ethanol : glacial acetic acid : water = 10 : 50 : 5 : 35) for at least 24 hours and washed in water for 24 ~ 48 hr. Then the samples were dehydrated in 50%, 60%, 70%, 80%, 90% ethanol series for 20 min once, and 100% ethanol for 20 min twice. The samples were incubated in a series of ethanol:xylene mix (75:25, 50:50, and 25:75) for 30 min in each mix, and to a series of xylene:paraffin mix (2:1, 1:1, and 1:2) for 1 hr twice in each mix. The samples were incubated in molten paraffin for 24 hr and poured into blocks on slide warmer at 70 °C and cooled down to 25 °C. Eight μ -thick transvers sections of paraffin-embedded samples were made with a microtome. Ribbons of serial sections floated on warm water (50 °C) were transferred to slide glasses on slide warmer at 70 °C and cooled down to 25 °C. Paraffin in the sections was removed with xylene.

4',6-diamidino-2-phenylindole (dapi) Staining Of Pollen Grains

For DAPI staining, pollens in 0 ~ 2 mm, 2 ~ 4 mm, 4 ~ 6 mm, 6 ~ 8 mm, and 8 ~ 10 mm TO1000 floral buds were put on microscope slides and stained with several drops of DAPI-staining solution, as described [66]. The pollen nuclei were inspected under Olympus BX51 fluorescence microscope (Tokyo, Japan) with a DAPI filter.

Abbreviations

GH3

Gretchen Hagen 3

bp

base pairs

qRT-PCR

quantitative reverse transcription polymerase chain reaction

GUS

β -glucuronidase

DAPI

4',6-diamidino-2-phenylindole

2,4-D

2,4-Dichlorophenoxy acetic acid

IAA

Indole-3-acetic acid

GA

Gibberellic acid 3

JA

Jasmonic acid

Declarations

Ethics approval and consent to participate

Not applicable

Consent for publication

Not applicable

Competing interests

The authors declare that they have no competing interests

Funding

This work was supported by Chungnam National University in Republic of Korea

Authors' contributions

JJ: designing and conducting of experiments, writing of manuscript

SP: conducting of experiments

Jl: conducting of experiments

HY: designing of experiments, writing of manuscript

Acknowledgements

The authors appreciate Yoonkang Hur, Jeong-Won Nam, Yeon Lee, Byugwook Kang, Jinouk Yeon, and Jaebeom Lim for their helpful discussions.

References

1. Hagen G, Kleinschmidt A, Guilfoyle T. Auxin-regulated gene expression in intact soybean hypocotyl and excised hypocotyl sections. *Planta*. 1984;162:147–53.
2. Hsieh HL, Okamoto H, Wang M, Ang LH, Matsui M, Goodman H, Deng XW. *FIN219*, an auxin regulated gene, defines a link between phytochrome A and the downstream regulator COP1 in light control of *Arabidopsis* development. *Genes Dev*. 2000;14:1958–70.
3. Ludwig-Müller J, Jülke S, Bierfreund NM, Decker EL, Reski R. Moss (*Physcomitrella patens*) GH3 proteins act in auxin homeostasis. *New Phytol*. 2009;181:323–38.
4. Okrent RA, Wildermuth MC. Evolutionary history of the GH3 family of acyl adenylases in rosids. *Plant Mol Biol*. 2011;76:489–505.
5. Roux C, Perrot-Rechenmann C. Isolation by differential display and characterization of a tobacco auxin-responsive cDNA Nt-gh3, related to GH3. *FEBS Lett*. 1997.
6. Yuan H, Zhao K, Lei H, Shen X, Liu Y, Liao X, Li T. Genome-wide analysis of the GH3 family in apple (*Malus × domestica*). *BMC Genom*. 2013;14:297.
7. Zhang C, Zhang L, Wang D, Ma H, Liu B, Shi Z, Ma X, Chen Y, Chen Q. Evolutionary history of the glycoside hydrolase 3 (GH3) family based on the sequenced genomes of 48 plants and identification of jasmonic acid-related GH3 proteins in *Solanum tuberosum*. *Int J Mol Sci*. 2018;19:1850.
8. Chen Q, Westfall CS, Hicks LM, Wang S, Jez JM. Kinetic basis for the conjugation of auxin by a GH3 family indole-acetic acid-amido synthetase. *J Biol Chem*. 2010;285:29780–6.
9. Gulick AM. Conformational dynamics in the acyl-CoA synthetases, adenylation domains of non-ribosomal peptide synthetases, and firefly luciferase. *ACS Chem Biol*. 2009;4:811–27.
10. Staswick PE, Tiryaki I, Rowe ML. Jasmonate response locus *JAR1* and several related *Arabidopsis* genes encode enzymes of the firefly luciferase superfamily that show activity on jasmonic, salicylic, and indole-3-acetic acids in an assay for adenylation. *Plant Cell*. 2002;14:1405–15.

11. Zheng Z, Guo Y, Novák O, Chen W, Ljung K, Noel JP, Chory J. Local auxin metabolism regulates environment-induced hypocotyl elongation. *Nat Plants*. 2016;2:16025.
12. Westfall CS, Zubieta C, Herrmann J, Kapp U, Nanao MH, Jez JM. Structural basis for prereceptor modulation of plant hormones by GH3 proteins. *Science*. 2012;336:1708–11.
13. Staswick PE, Tiryaki I. The oxylipin signal jasmonic acid is activated by an enzyme that conjugates it to isoleucine in Arabidopsis. *Plant Cell*. 2004;16:2117–27.
14. Torrens-Spence MP, Bobokalonova A, Carballo V, Glinkerman CM, Pluskal T, Shen A, Weng JK. PBS3 and EPS1 complete salicylic acid biosynthesis from isochorismate in Arabidopsis. *Mol Plant*. 2019;12:1577–86.
15. Nakazawa M, Yabe N, Ichikawa T, Yamamoto YY, Yoshizumi T, Hasunuma K, Matsui M. *DFL1*, an auxin-responsive *GH3* gene homologue, negatively regulates shoot cell elongation and lateral root formation, and positively regulates the light response of hypocotyl length. *Plant J*. 2001;25:213–21.
16. Takase T, Nakazawa M, Ishikawa A, Kawashima M, Ichikawa T, Takahashi N, Shimada H, Manabe K, Matsui M. *ydk1-D*, an auxin-responsive GH3 mutant that is involved in hypocotyl and root elongation. *Plant J*. 2004;37(4):471–83.
17. Park JE, Park JY, Kim YS, Staswick PE, Jeon J, Yun J, Kim SY, Kim J, Lee YH, Park CM. GH3-mediated auxin homeostasis links growth regulation with stress adaptation response in Arabidopsis. *J Biol Chem*. 2007;282:10036–46.
18. Damodaran S, Westfall CS, Kisely BA, Jez JM, Subramanian S. Nodule-enriched GRETCHEN HAGEN 3 enzymes have distinct substrate specificities and are important for proper soybean nodule development. *Int J Mol Sci*. 2017;18:E2547.
19. Zou X, Long J, Zhao K, Peng A, Chen M, Long Q, He Y, Chen S. Overexpressing *GH3.1* and *GH3.1L* reduces susceptibility to *Xanthomonas citri* subsp. *citri* by repressing auxin signaling in citrus (*Citrus sinensis* Osbeck). *PLoS One*. 2019;14:e0220017.
20. Kirungu JN, Magwanga RO, Lu P, Cai X, Zhou Z, Wang X, Peng R, Wang K, Liu F. Functional characterization of *Gh_A08G1120* (*GH3.5*) gene reveal their significant role in enhancing drought and salt stress tolerance in cotton. *BMC Genet*. 2019;20:62.
21. Gan Z, Fei L, Shan N, Fu Y, Chen J. Identification and expression analysis of *Gretchen Hagen 3* (*GH3*) in Kiwifruit (*Actinidia chinensis*) during postharvest process. *Plants (Basel)*. 2019;8:473.
22. Okrent RA, Brooks MD, Wildermuth MC. Arabidopsis. GH3.12 (PBS3) conjugates amino acids to 4-substituted benzoates and is inhibited by salicylate. *J Biol Chem*. 2009;284:9742–54.
23. Sravankumar T, Akash, Naik N, Kumar R. A ripening-induced *SIGH3-2* gene regulates fruit ripening via adjusting auxin-ethylene levels in tomato (*Solanum lycopersicum* L.). *Plant Mol Biol*. 2018;98:455–69.
24. Feng S, Yue R, Tao S, Yang Y, Zhang L, Xu M, Wang H, Shen C. Genome-wide identification, expression analysis of auxin-responsive *GH3* family genes in maize (*Zea mays* L.) under abiotic stresses. *J Integr Plant Biol*. 2015;57:783–95.

25. Jain M, Kaur N, Tyagi AK, Khurana JP. The auxin-responsive *GH3* gene family in rice (*Oryza sativa*). *Funct Integr Genomics*. 2006;6:36–46.
26. Kong W, Zhang Y, Deng X, Li S, Zhang C, Li Y. Comparative genomic and transcriptomic analysis suggests the evolutionary dynamic of *GH3* Genes in *Gramineae* crops. *Front Plant Sci*.
27. Holland CK, Westfall CS, Schaffer JE, De Santiago A, Zubieta C, Alvarez S, Jez JM. *Brassicaceae*-specific Gretchen Hagen 3 acyl acid amido synthetases conjugate amino acids to chorismate, a precursor of aromatic amino acids and salicylic acid. *J Biol Chem*. 2019;294:16855–64.
28. Peat TS, Böttcher C, Newman J, Lucent D, Cowieson N, Davies C. Crystal structure of an indole-3-acetic acid amido synthetase from grapevine involved in auxin homeostasis. *Plant Cell*. 2012;24:4525–38.
29. Sherp AM, Westfall CS, Alvarez S, Jez JM. Arabidopsis *thaliana* GH3.15 acyl acid amido synthetase has a highly specific substrate preference for the auxin precursor indole-3-butyric acid. *J Biol Chem*. 2018;293:4277-88.
30. Staswick PE, Serban B, Rowe M, Tiryaki I, Maldonado MT, Maldonado MC, Suza W. Characterization of an Arabidopsis enzyme family that conjugates amino acids to indole-3-acetic acid. *Plant Cell*. 2005;17:616–27.
31. Westfall CS, Sherp AM, Zubieta C, Alvarez S, Schraft E, Marcellin R, Ramirez L, Jez JM. Arabidopsis *thaliana* GH3.5 acyl acid amido synthetase mediates metabolic crosstalk in auxin and salicylic acid homeostasis. *Proc Natl Acad Sci USA*. 2016;113(48):13917–22.
32. Chiu LW, Heckert MJ, You Y, Albanese N, Fenwick T, Siehl DL, Castle LA, Tao Y. Members of the GH3 family of proteins conjugate 2,4-D and dicamba with aspartate and glutamate. *Plant Cell Physiol*. 2018;59:2366–80.
33. Wang R, Li M, Wu X, Wang J. The gene structure and expression level changes of the *GH3* Gene family in *Brassica napus* relative to its diploid ancestors. *Genes (Basel)*. 2019;10:58.
34. Wei L, Yang B, Jian H, Zhang A, Liu R, Zhu Y, Ma J, Shi X, Wang R, Li J, Xu X. Genome-wide identification and characterization of *Gretchen Hagen3 (GH3)* family genes in *Brassica napus*. *Genome* 2019;62:597–608.
35. Parkin IA, Koh C, Tang H, Robinson SJ, Kagale S, Clarke WE, et al. Transcriptome and methylome profiling reveals relics of genome dominance in the mesopolyploid *Brassica oleracea*. *Genome Biol*. 2014;15:R77.
36. Goldberg RB, Beals TP, Sanders PM. Anther development: basic principles and practical applications. *Plant Cell*. 1993;5:1217–29.
37. Marciniak K, Przedniczek K. Comprehensive Insight into gibberellin- and jasmonate-mediated stamen development. *Genes (Basel)*. 2019;10.
38. Borg M, Brownfield L, Twell D. Male gametophyte development: a molecular perspective. *J Exp Bot*. 2009;60:1465–78.
39. Scott RJ, Spielman M, Dickinson HG. Stamen structure and function. *Plant Cell*. 2004;16:46–60.

40. Yamamoto Y, Nishimura M, Hara-Nishimura I, Noguchi T. Behavior of vacuoles during microspore and pollen development in *Arabidopsis thaliana*. *Plant Cell Physiol*. 2003;44:1192–201.
41. Williams JH, Taylor ML, O'Meara BC. Repeated evolution of tricellular (and bicellular) pollen. *Am J Bot*. 2014;101:559–71.
42. Acosta IF, Przybyl M. Jasmonate signaling during Arabidopsis stamen maturation. *Plant Cell Physiol*. 2019;60:2648–59.
43. Schubert R, Grunewald S, von Sivers L, Hause B. Effects of jasmonate on ethylene function during the development of tomato stamens. *Plants (Basel)*. 2019;8:E277.
44. Yao X, Tian L, Yang J, Zhao YN, Zhu YX, Dai X, Zhao Y, Yang ZN. Auxin production in diploid microsporocytes is necessary and sufficient for early stages of pollen development. *PLoS Genet*. 2018;14:e1007397.
45. Koltunow AM, Truettner J, Cox KH, Wallroth M, Goldberg RB. Different temporal and spatial gene expression patterns occur during anther development. *Plant Cell*. 1990;2:1201–24.
46. Ma H. Molecular genetic analyses of microsporogenesis and microgametogenesis in flowering plants. *Annu Rev Plant Biol*. 2005;56:393–434.
47. Twell D. Male gametogenesis and germline specification in flowering plants. *Sex Plant Reprod*. 2011;24:149–60.
48. Liu S, Liu Y, Yang X, Tong C, Edwards D, Parkin IA, et al. The *Brassica oleracea* genome reveals the asymmetrical evolution of polyploid genomes. *Nat Commun*. 2014;5:3930.
49. Panchy N, Lehti-Shiu M, Shiu SH. Evolution of Gene Duplication in Plants. *Plant Physiol*. 2016;171:2294–316.
50. Pearce S, Ferguson A, King J, Wilson ZA. FlowerNet: a gene expression correlation network for anther and pollen development. *Plant Physiol*. 2015;167:1717–30.
51. Sanders PM, Bui AQ, Weterings K, McIntire KN, Hsu Y, Lee PY, Truong MT, Beals TP, Goldberg RB. Anther developmental defects in *Arabidopsis thaliana* male-sterile mutants. *Sex Plant Reprod*. 1999;11:297–322.
52. Yang Y, Yue R, Sun T, Zhang L, Chen W, Zeng H, Wang H, Shen C. Genome-wide identification, expression analysis of GH3 family genes in *Medicago truncatula* under stress-related hormones and *Sinorhizobium meliloti* infection. *Appl Microbiol Biotechnol*. 2015;99:841–54.
53. Yu D, Qanmber G, Lu L, Wang L, Li J, Yang Z, Liu Z, Li Y, Chen Q, Mendu V, Li F, Yang Z. Genome-wide analysis of cotton *GH3* subfamily II reveals functional divergence in fiber development, hormone response and plant architecture. *BMC Plant Biol*. 2018;18:350.
54. Basu MM, González-Carranza ZH, Azam-Ali S, Tang S, Shahid AA, Roberts JA. The manipulation of auxin in the abscission zone cells of Arabidopsis flowers reveals that indoleacetic acid signaling is a prerequisite for organ shedding. *Plant Physiol*. 2013;162:96–106.
55. Cecchetti V, Altamura MM, Falasca G, Costantino P, Cardarelli M. Auxin regulates Arabidopsis anther dehiscence, pollen maturation, and filament elongation. *Plant Cell*. 2008;20:1760–74.

56. Cecchetti V, Celebrin D, Napoli N, Ghelli R, Brunetti P, Costantino P, Cardarelli M. An auxin maximum in the middle layer controls stamen development and pollen maturation in *Arabidopsis*. *New Phytol.* 2017;213:1194–207.
57. Yang J, Yuan Z, Meng Q, Huang G, Périn C, Bureau C, Meunier AC, Ingouff M, Bennett MJ, Liang W, Zhang D. Dynamic regulation of auxin response during rice development revealed by newly established hormone biosensor markers. *Front Plant Sci.* 2017;8:256.
58. Gómez JF, Talle B, Wilson ZA. Anther and pollen development: A conserved developmental pathway. *J Integr Plant Biol.* 2015;57:876–91.
59. Chow C, Zheng H, Wu N, Chien C, Huang H, Lee T, Chiang-Hsieh Y, Hou P, Yang T, Chang W. PlantPAN 2.0: an update of plant promoter analysis navigator for reconstructing transcriptional regulatory networks in plants. *Nucleic Acids Res.* 2015;44:D1154-60.
60. Yu J, Zhao M, Wang X, Tong C, Huang S, Tehrim S, Liu Y, Hua W, Liu S. Bolbase: a comprehensive genomics database for *Brassica oleracea*. *BMC Genom.* 2013;14:664.
61. Sievers F, Wilm A, Dineen D, Gibson TJ, Karplus K, Li W, Lopez R, McWilliam H, Remmert M, Söding J, Thompson JD, Higgins DG. Fast, scalable generation of high-quality protein multiple sequence alignments using Clustal Omega. *Mol Syst Biol.* 2011;7:539.
62. Waterhouse AM, Procter JB, Martin DM, Clamp M, Barton GJ. Jalview Version 2– a multiple sequence alignment editor and analysis workbench. *Bioinformatics.* 2009;25:1189–91.
63. Kumar S, Stecher G, Li M, Knyaz C, Tamura K. MEGA X: Molecular evolutionary genetics analysis across computing platforms. *Mol Biol Evol.* 2018;35:1547–49.
64. Jones DT, Taylor WR, Thornton JM. The rapid generation of mutation data matrices from protein sequences. *Bioinformatics.* 1992;8:275–82.
65. Clough SJ, Bent AF. Floral dip: a simplified method for *Agrobacterium*-mediated transformation of *Arabidopsis thaliana*. *Plant J.* 1998;16:735–43.
66. Hong J, Lee J, Jeong CW, Brooks JS, Choi Y, Lee JS. Characteristics and regulating role in thermotolerance of the heat shock transcription factor ZmHsf12 from *Zea mays L.* *J. Plant Biol.*
67. Dong X, Nou IS, Yi H, Hur Y. Suppression of *ASKβ* (*AtSK32*), a clade III *Arabidopsis GSK3*, leads to the pollen defect during late pollen development. *Mol Cells.* 2015;38:506–17.

Figures

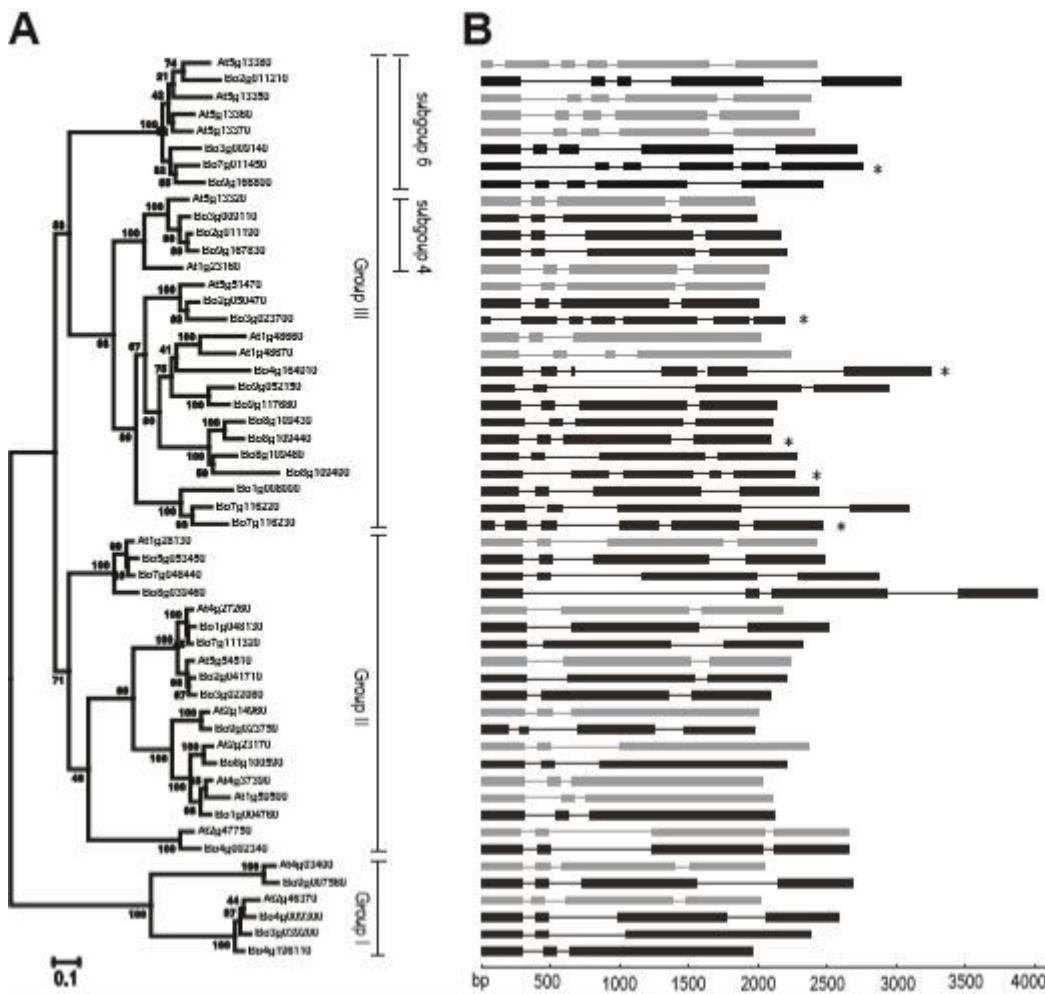


Figure 1

Phylogenetic relationships and exon/intron structures of GH3 proteins in Arabidopsis and TO1000. (A) Phylogenetic analysis of GH3 family members in Arabidopsis and TO1000. The percentage of trees in which the associated taxa clustered together is shown next to the branches. The phylogenetic tree is drawn to scale, with branch lengths measured in the number of substitutions per site. Bootstrap test percentages of 1000 replicates are shown next to the branches. (B) Gene structures for Arabidopsis and TO1000 GH3 proteins were generated by gene structure display servers (http://gsds.cbi.pku.edu.cn/Gsds_about.php). Note that exons indicated here do not contain untranslated regions. Asterisks indicate exon/intron structures of genes, which were annotated only in Ensembl Plants. The black boxes and lines represent exons and introns in TO1000 GH3 genes, while the gray boxes and lines represent exons and introns in Arabidopsis GH3 genes. Groups (I~III) and subgroups (4 & 6) of GH3 proteins were designated based on the Staswick et al. (2002) and Westfall et al. (2012), respectively [10,12].

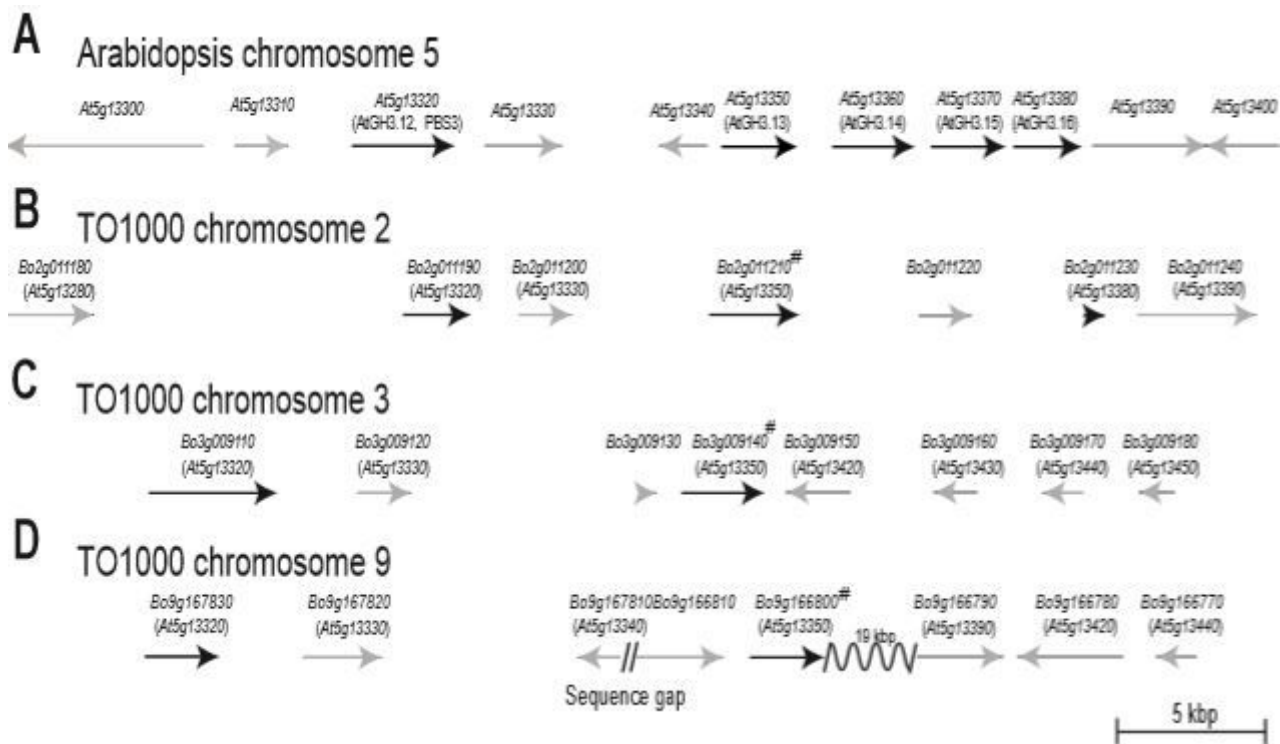


Figure 2

Synteny is found between genomic regions around Arabidopsis At5g13350 and corresponding regions in TO1000. Each panel shows gene organization, in which GH3 and non-GH3 genes from start to stop codons are indicated by black and gray arrows, respectively. Direction of each arrow shows that of gene transcription. (A) The gene organization on Arabidopsis chromosome 5 around At5g13350. (B-D) The gene organizations of TO1000 chromosome 2 near Bo2g011210, chromosome 3 near Bo3g009140, and chromosome 9 near Bo9g166800. Arabidopsis genes showing sequence similarities to TO1000 genes are indicated in parenthesis below TO1000 gene names. The TO1000 BoGH3 genes similar to Arabidopsis At5g13350~ At5g13380 GH3 gene cluster are indicated with sharp (#) symbols. Bo2g011230 in (B) encodes a truncated protein with a sequence similarity to Arabidopsis GH3 genes in the cluster.

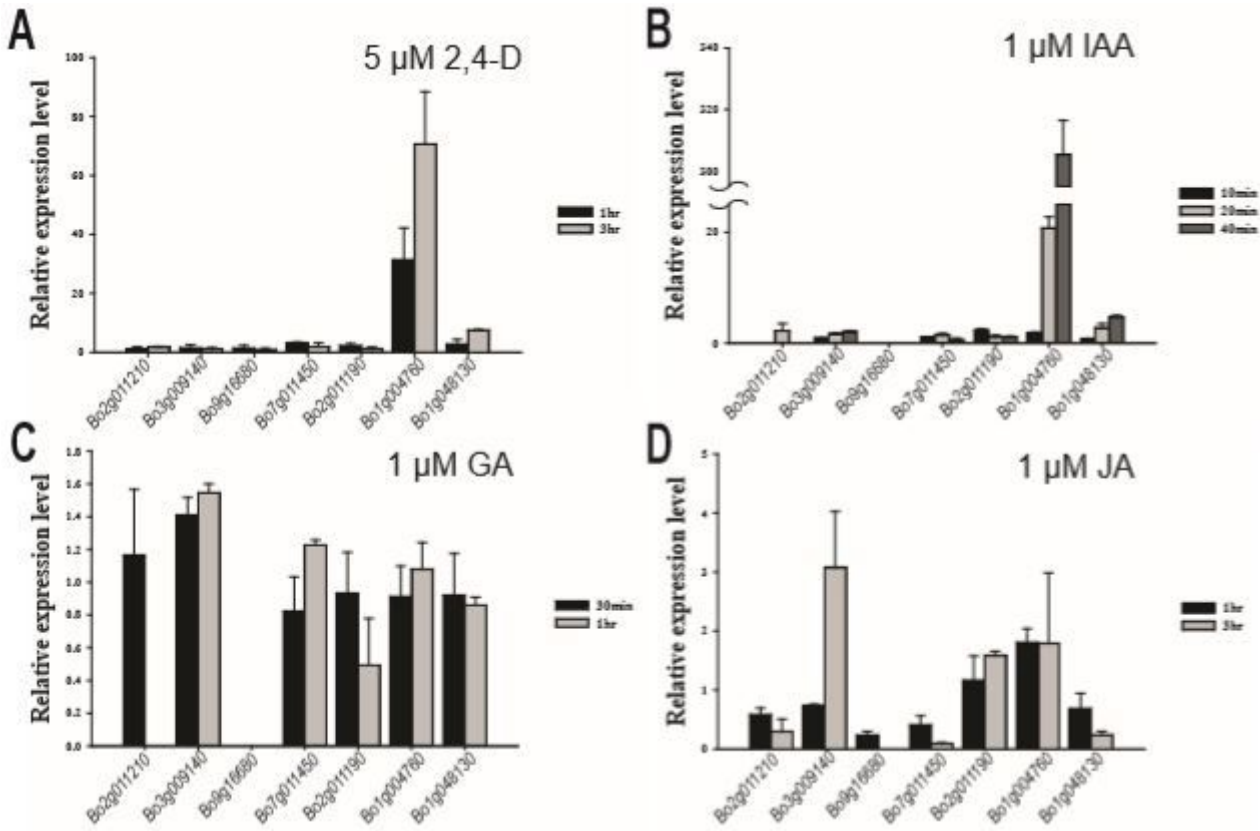


Figure 3

Subgroup 6 BoGH3 genes are not induced by auxin at the seedling stage. Relative expression levels of four subgroup 6 BoGH3 genes and two other selected GH3 genes were determined by qRT-PCR experiment with Actin control. The expression level of mock condition was set to value 1 and used as reference to compare expression level changes after hormone treatments. Bar graphs show average relative expression values with standard errors (SE). Averages values of two independent results for 2,4-D or JA treatments are shown, while representative results are shown for IAA or GA treatments. Bar graphs for genes without any significant amplification are not included.

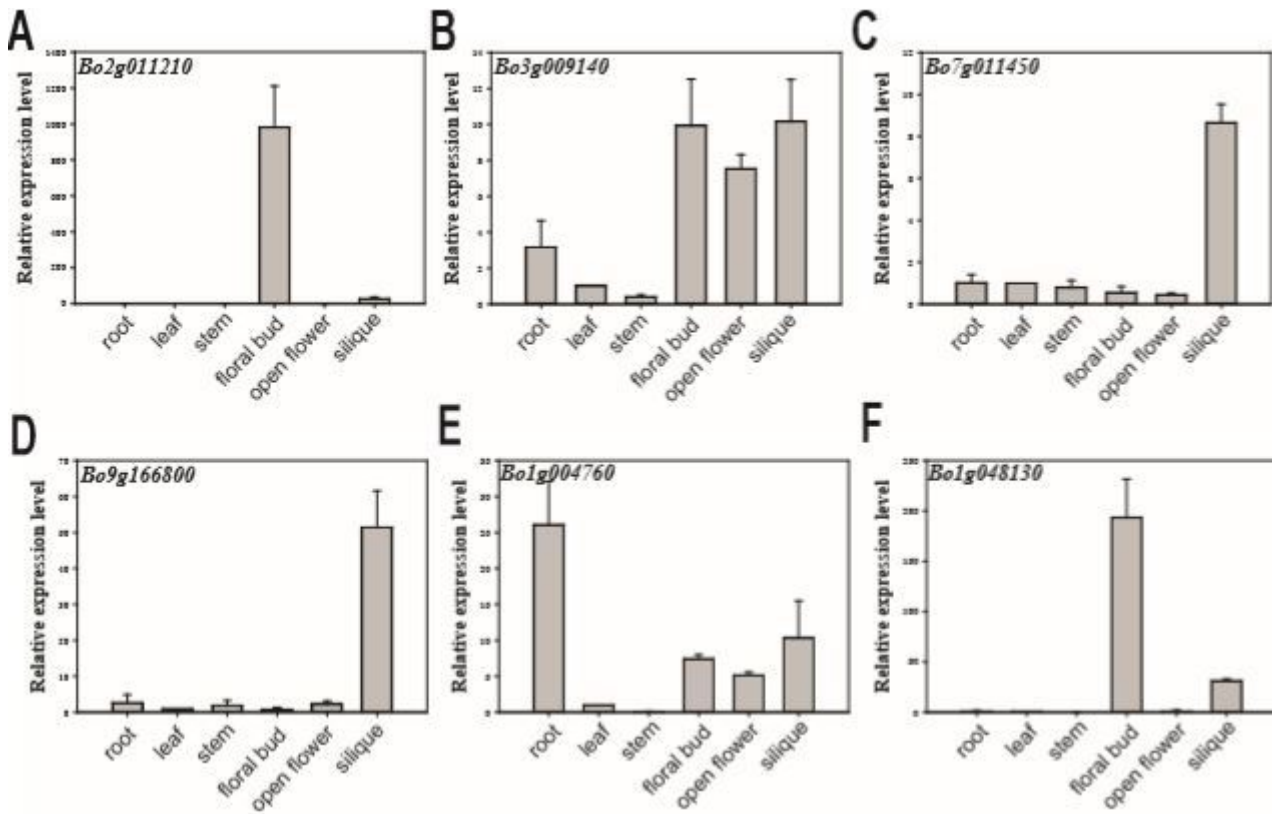


Figure 4

qRT-PCR results showing expression patterns of selected BoGH3 genes in different organs. Relative steady-state expression levels of some BoGH3 genes were determined by qRT-PCR experiment with Actin control. Bar graphs show average relative expression values with SEs. The expression level of leaf was set to value 1 and used as reference to compare expression levels in different organs.

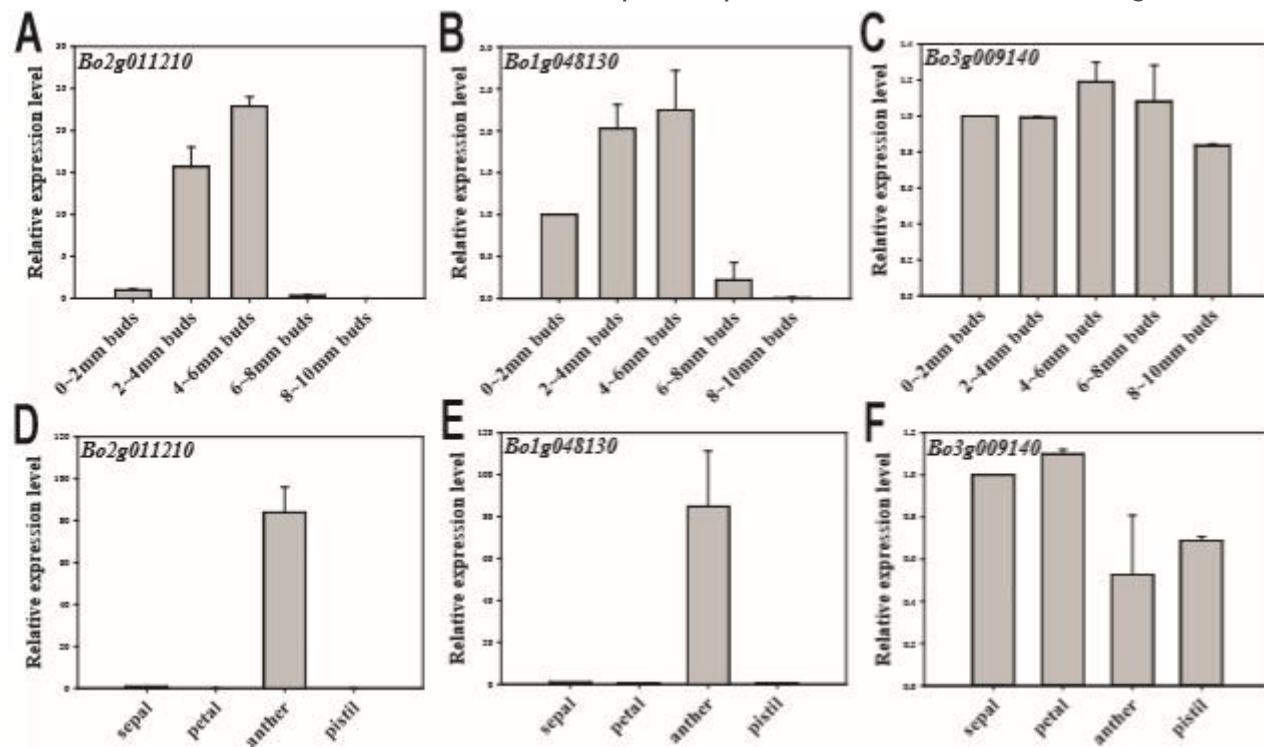


Figure 5

Bo2g011210 and Bo1g048130 are strongly expressed in anther. Steady-state expression levels of selected BoGH3 genes, which are expressed in unopened floral bud, were determined with qRT-PCR. Bar graphs show average relative expression values with SEs. The expression level of 0 ~ 2 mm buds (A-C) and that of sepal (D-E), which were normalized to that of ACTIN, were set to value 1 and used as reference.

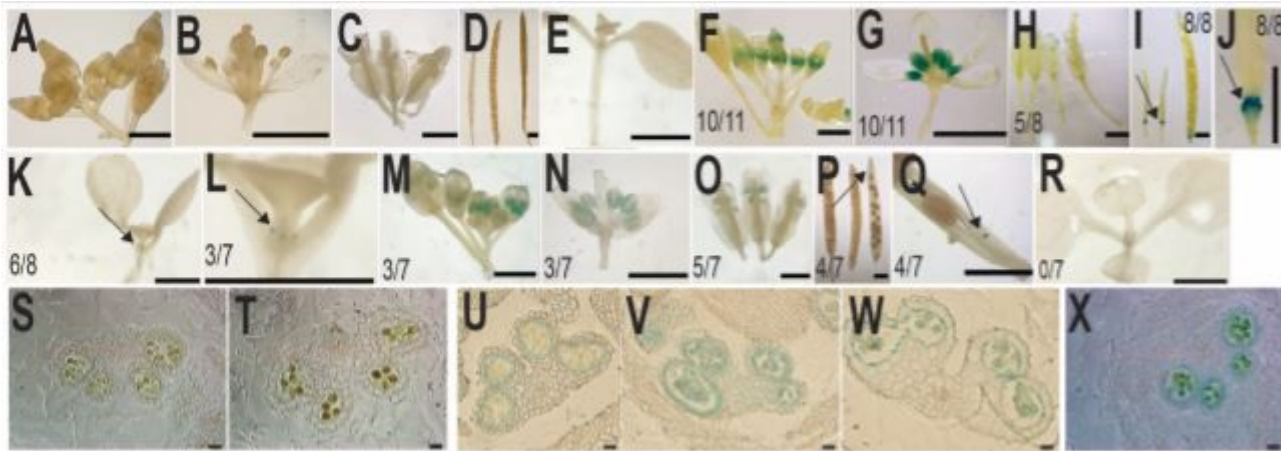


Figure 6

GUS staining patterns in *Arabidopsis* transgenic plants with two BoGH3 promoter::GUS transgene. (A-E) samples from wild-type *Arabidopsis* plants (WT) - floral buds (A), a dissected floral bud (B), open flowers (C), siliques (D), and 8-day old seedling (E). (F-L) samples from Bo2g011210 (-1489 ~ -1)::GUS transgenic plants - floral buds (F), a dissected floral bud (G), open flowers (H), siliques (I-J), and 8-day old seedling (K-L). (M-R) samples from Bo1g048130 (-1496 ~ -1)::GUS transgenic - floral buds (M), a dissected floral bud (N), open flowers (O), siliques (P-Q), and 8-day old seedling (R). Transverse sections of GUS-stained floral buds of WT plants (S-T). Transverse sections of GUS-stained floral buds of Bo2g011210 (-1489 ~ -1)::GUS (U-W). Transverse sections of GUS-stained floral buds of Bo1g048130 (-1496 ~ -1)::GUS (X). Dividends and denominators of fractions in the pictures are transgenic plants with the GUS staining and all the transgenic plants examined, respectively. Arrows indicate GUS stained parts. Scale bars in A-R: 1 mm. Scale bars in S-X: 20 μ m.

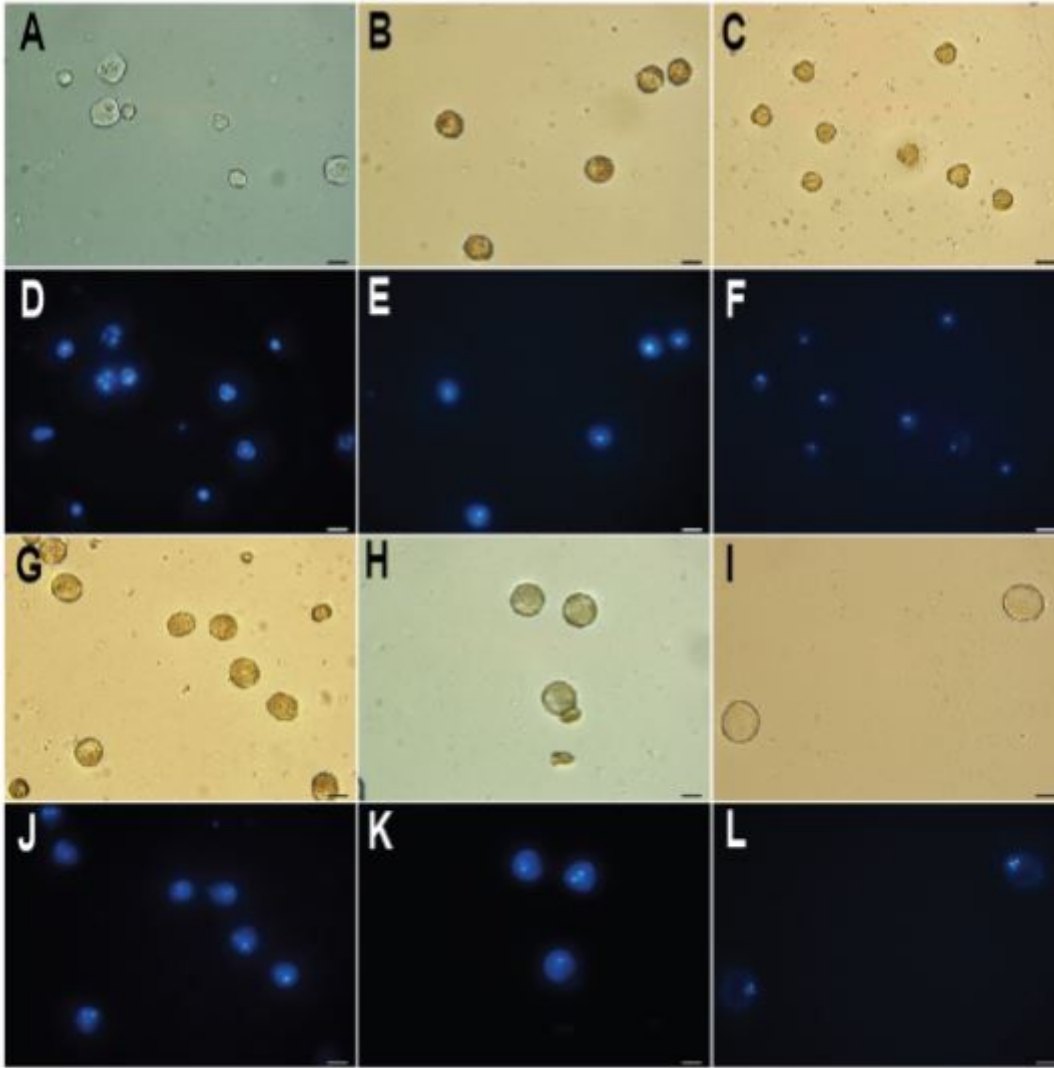


Figure 7

DAPI-stained developing pollen grains in TO1000 floral buds. Bright-field images of pollens in less than 2 \times floral buds (A), 2 \sim 4 \times buds (B), 4 \sim 6 mm buds (C), 6 \sim 8 \times buds (G), 8 \sim 10 \times buds (H), and open flowers (I). Fluorescence images of DAPI-stained pollens in less than 2 \times floral buds (D), 2 \sim 4 \times buds (E), 4 \sim 6 mm buds (F), 6 \sim 8 \times buds (J), 8 \sim 10 \times buds (K), and open flowers (L). Scale bar: 20 μ .

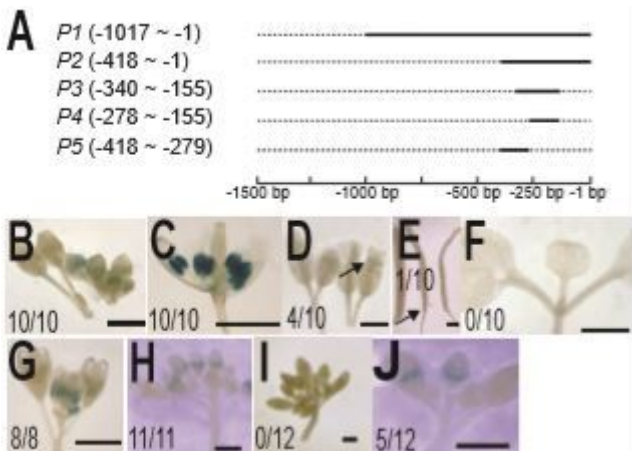


Figure 8

Representative GUS staining patterns to define a promoter region directing anther-specific expression of Bo2g11210. (A) Genomic DNA regions used in transgenic lines for promoter analysis. Names of transgenic plants used are written in *italic* and different regions upstream of Bo2g011210 start codon to direct GUS reporter expression are indicated in parentheses. (B-F) GUS staining of floral buds (B), a dissected floral bud (C), open flowers (D), siliques (E), and 8-day old seedling (F) of P1 transgenic plants, and floral buds from P2 (G), P3 (H), P4 (I), and P5 (J) are shown. Arrows indicate GUS-stained pollen (D) or floral abscission zones in a silique (E), respectively. Dividends and denominators of fractions in the pictures are numbers of transgenic plants with the GUS staining and all the transgenic plants examined, respectively. Scale bars: 1 mm.

Supplementary Files

This is a list of supplementary files associated with this preprint. Click to download.

- [TableS4Boleraceacapitata.docx](#)
- [TableS3GUSPromoterPrimer.docx](#)
- [TableS2qRT-PCRPrimers.docx](#)
- [TableS1BoleraceaoLERACEA.docx](#)
- [FigS2FloralBuds.pdf](#)
- [FigS1Bo34SeqAlign.pdf](#)